American Mineralogist, Volume 70, pages 1262–1269, 1985

Electronic spectra of Fe^{3+} oxides and oxide hydroxides in the near IR to near UV

DAVID M. SHERMAN[1]

Department of Earth, Atmospheric and Planetary Sciences
Massachusetts Institute of Technology, Cambridge, MA 02139

AND T. DAVID WAITE[2]

Department of Civil Engineering
Massachusetts Institute of Technology, Cambridge, MA 02319

Abstract

Optical absorption and diffuse reflectance spectra of several Fe_2O_3 and FeOOH polymorphs (hematite, maghemite, goethite, lepidocrocite) in the near-infrared to near-ultraviolet spectral regions (2000–200 nm) are presented. The spectra consist primarily of Fe^{3+} ligand field and ligand to metal charge-transfer transitions. Band assignments were made using ligand field theory and the results of recent SCF-Xα-SW molecular orbital calculations of $(FeO_6)^{9-}$ coordination polyhedra. Values of the ligand field parameters $10Dq$, B and C were found to be 14000–15900, 550–610, and 3400–3500 cm^{-1}, respectively. The lowest energy ligand-to-metal charge-transfer transition is near 40,000 cm^{-1} in agreement with the molecular orbital calculations. The Fe^{3+} ligand field transitions are strongly intensified by magnetic coupling of adjacent Fe^{3+} cations. Several additional spectral bands are assigned to "double exciton" processes involving the simultaneous excitation of two Fe^{3+} cations which are magnetically coupled. These results show that the red to yellow colors of these minerals are not due to the LMCT transitions but result from pair excitations and Fe^{3+} ligand field transitions which have been intensified by magnetic coupling of adjacent Fe^{3+} cations.

Introduction

The electronic spectra of iron oxides and oxide hydroxides are directly relevant to several current problems in geochemistry. At present, a great deal of interest in planetary science is directed towards determining the surface mineralogy of Mars using spectroscopic remote sensing techniques (e.g., Singer et al., 1979; Singer, 1982; Sherman et al., 1982). On another front, the electronic transitions which give iron(III) oxides their optical spectra are also of interest in that they determine the mechanisms of sunlight-induced photochemical reactions between colloidal iron oxides and organic molecules in natural waters (Waite, 1983). Although several of the iron oxides and oxide hydroxides (e.g., hematite and goethite) are among the most common minerals on the Earth's surface, their electronic spectra are poorly known or understood. As will be discussed below, the spectra of Fe^{3+} minerals consist not only of electronic transitions localized to the FeO_6 coordination site (e.g., Fe^{3+} ligand field and $O^{2-} \rightarrow Fe^{3+}$ charge-transfer transitions) but can also exhibit phenomena resulting from the interactions between adjacent Fe^{3+} cations. These latter phenomena make the spectra of condensed Fe^{3+} phases (such as iron oxides) considerably more complex than those of dilute Fe^{3+} cations in a silicate or oxide host phase.

In this paper, the near-IR to near-UV electronic spectra of hematite (α-Fe_2O_3), maghemite (γ-Fe_2O_3), goethite (α-FeOOH) and lepidocrocite (γ-FeOOH) are presented. An earlier study of the diffuse reflectance spectra of these phases has been done by Strens and Wood (1979) but specific band assignments were not made. In this paper, detailed band assignments will be given based on ligand field theory, results of recent SCF-Xα-SW molecular orbital calculations (Sherman, 1985), and comparison with existing spectra of Fe^{3+} cations in oxides.

Theory of Fe^{3+} spectra in minerals

To help clarify the rationale behind the spectral band assignments, it is worthwhile to first review the important theoretical aspects of Fe^{3+} electronic spectra in minerals. Three types of electronic transitions occur in the optical spectra of Fe^{3+} minerals. First, there are the Fe^{3+} ligand field transitions; second, there are the ligand to metal charge-transfer transitions; and, third, there are transitions which result from the simultaneous excitation of

[1] Present Address: U.S. Geological Survey, 959 National Center, Reston, Virginia 22092.

[2] Present Address: School of Chemistry, University of Melbourne, Parkville, Victoria, Australia 3052.

0003–004X/85/1112–1262$02.00

Table 1. Tanabe–Sugano expressions for the ligand field state energies of octahedral Fe^{3+} (from Lever, 1968). The terms which are quadratic in B describe the configurational interaction and are derived assuming $C = 4B$. The quantities designated by x in the expressions for the $^4T_2(^4D)$ and $^4T_1(^4P)$ state energies arise from off-diagonal elements in the Tanabe–Sugano matrices; these quantities are neglected in the calculations of the spectroscopic state energies (Table 2).

State	Configuration	Energy
$^4T_1(^4G)$	$(t_{2g})^4(e_g)^1$	$-10Dq + 10B + 6C - 26B^2/10Dq$
$^4T^2(^4G)$	$(t_{2g})^4(e_g)^1$	$-10Dq + 18B + 6C - 38B^2/10Dq$
$^4E,^4A_1(^4G)$	$(t_{2g})^3(e_g)^2$	$10B + 5C$
$^4T_2(^4D)$	$(t_{2g})^3(e_g)^2$	$13B + 5C + x$
$^4E(^4D)$	$(t_{2g})^3(e_g)^2$	$17B + 5C$
$^4T_1(^4P)$	$(t_{2g})^3(e_g)^2$	$19B + 7C - x$
$^4A_2(^4F)$	$(t_{2g})^3(e_g)^2$	$22B + 7C$

magnetically-coupled Fe^{3+} cations which occupy adjacent sites.

Fe^{3+} ligand field transitions

In octahedral coordination, the Fe(3*d*) atomic orbitals are split into two sets of orbitals labelled t_{2g} and e_g. The t_{2g} and e_g orbital energy separation is the $10Dq$ ligand field parameter or the crystal field splitting. The t_{2g} and e_g orbitals are each split, in turn, by the exchange energy. The latter is the stabilization of electrons with majority spin (α-spin). The exchange splitting results in two sets of t_{2g} and e_g orbitals, one for the majority spin (spin-up or α-spin) and the other for minority spin (spin-down or β-spin) electrons. The Racah B and C parameters of ligand field theory are, in effect, measures of the exchange splitting of the t_{2g} and e_g orbitals. The ligand field transitions are between the states which arise from the different possible electronic configurations of the t_{2g} and e_g orbitals. In the approximation of ligand field theory, the energies of these states are expressed in terms of the three parameters $10Dq$, B and C. Analytical expressions for these state energies, which will be used to make spectral band assignments, are given in Table 1. The energies of the Fe^{3+} ligand field states as a function of $10Dq$ (assuming constant B and C) are shown schematically in the Tanabe–Sugano diagram in Figure 1 (this was calculated using the expressions in Table 1).

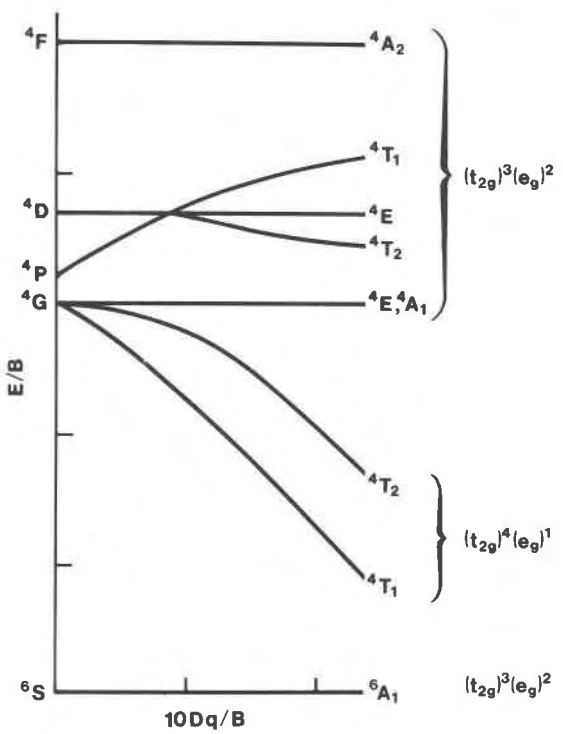

Fig. 1. Tanabe–Sugano diagram for high-spin Fe^{3+} in either octahedral or tetrahedral coordination. The state energies as a function of $10Dq$ were calculated using the expressions in Table 1 and assuming $C/B = 4$.

The ground $^6A_1(^6S)$ state in Figure 1 arises from the ground state $(t^{\alpha}_{2g})^3(e^{\alpha}_g)^2$ configuration of high-spin Fe^{3+}. The first possible excited state configuration is $(t^{\alpha}_{2g})^3(e^{\alpha}_g)^1(t^{\beta}_{2g})^1$. This configuration gives the $^4T_1(^4G)$ and $^4T_2(^4G)$ states of Figure 1. Note that the configuration giving these states contains singly occupied t^{β}_{2g} and e^{α}_g orbitals. Hence, it is expected that the $^4T_1(^4G)$ and $^4T_{2g}(^4G)$ states will each be split by the dynamic Jahn–Teller effect. The remaining states in Figure 1 result from the "spin-flip" configurations $(t^{\alpha}_{2g})^2(t^{\beta}_{2g})^1(e^{\alpha}_g)^2$ and $(t^{\alpha}_{2g})^3(e^{\alpha}_g)^1(e^{\beta}_g)^1$. Note that the energies of these configurations, relative to that of the ground configuration, are not a function of $10Dq$ but only of the exchange splittings of the t_{2g} and e_g orbitals. The latter are a function of the covalency of the Fe–O bond; as such, the energies of the states arising from these configurations are expected to fairly be constant among Fe^{3+} oxides and silicates.

All of the transitions from the ground $^6A_1(^6S)$ state to the excited ligand field states are, in principle, both spin- and parity-forbidden. In a number of Fe^{3+} minerals and binuclear inorganic complexes, however, these transitions become allowed through the magnetic coupling of electronic spins of next-nearest neighbor Fe^{3+} cations in the crystal structure (Ferguson et al., 1966; Krebs and Maisch, 1971; Lohr, 1972). If two Fe^{3+} cations are strongly coupled, one must consider the spectroscopic selection rules for the Fe^{3+}–Fe^{3+} pairs and not those for individual Fe^{3+} centers. We can obtain a qualitative understanding of the states associated with an Fe–Fe pair by assuming that the coupling between the two Fe centers is via the Heisenberg Hamiltonian:

$$\mathbf{H} = J\mathbf{S}_a \cdot \mathbf{S}_b \qquad (1)$$

Here, $\mathbf{S}_a$ and $\mathbf{S}_b$ are the electronic spins of the two Fe^{3+} cations and J is the Heisenberg exchange integral. Application of this Hamiltonian as a perturbation to the ligand field states of the uncoupled Fe^{3+} cations yields a set of

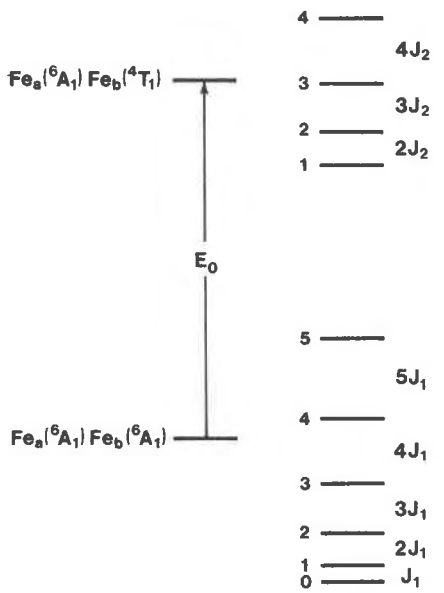

Fig. 2. States of an Fe^{3+}–Fe^{3+} pair assuming that the Fe^{3+} cations are coupled via the Heisenberg Hamiltonian $\mathbf{H} = J\mathbf{S}_a \cdot \mathbf{S}_b$. Here, J is the exchange integral, $\mathbf{S}_a$ and $\mathbf{S}_b$ are the net spins of Fe atoms a and b, E_0 is the energy difference between the ground $^6A_1$ state and an arbitrary quartet state of an isolated, uncoupled Fe^{3+} cation. The numbers next to each level indicate the spin quantum number (S) of the pair state.

states for the pair with energies given by

$$E = (J/2)[S(S+1) - S_a(S_a+1) - S_b(S_b+1)] \qquad (2)$$

where S is the net spin of the pair with values $|S_a + S_b|$, $|S_a + S_b - 1|, \ldots, |S_a - S_b|$. If both Fe^{3+} cations are in their ground $^6A_1$ states, then $S_a = S_b = 5/2$; the resulting pair-states derived by coupling the two Fe^{3+} cations will have $S = 0$, 1, 2, 3, 4, and 5. Now, if one of the Fe^{3+} cations in the pair is excited to a quartet ligand field state, then $S_a = 3/2$ and $S_b = 5/2$; the two Fe^{3+} cations would therefore couple to give a set of pair states with $S = 1$, 2, 3, and 4. Transitions from $S = 1$, 2, 3, and 4 states in the $Fe^{3+}(^6A_1)$–$Fe^{3+}(^6A_1)$ pair-state manifold to the states in the excited-single-ion pair-state manifold can, therefore, occur with $\Delta S = 0$ and be spin-allowed. The relative energies of the states in the ground and excited-single-ion pair-state manifolds are shown in Figure 2.

Pair excitations or double exciton processes

An additional phenomenon resulting from the magnetic coupling of adjacent Fe^{3+} cations is the presence of new absorption features corresponding to the simultaneous excitation of two Fe^{3+} centers (Schugar et al., 1972). These features occur at energies given approximately by the sum of two single ion Fe^{3+} ligand field transitions and are often referred to as "double exciton processes". Several absorption bands in the spectrum of Fe^{3+} cations in Al_2O_3 have been demonstrated by Ferguson and Fielding (1972) to result from these Fe^{3+}–Fe^{3+} pair excitations. These transitions are also spin-allowed: if both Fe^{3+} cations are excited to a quartet ligand field state so that $S_a = S_b = 3/2$, the pair states resulting from coupling the two Fe^{3+} cations will have S values of 0, 1, 2, and 3. Transitions to these pair states can therefore occur from the $S = 0$, 1, 2, and 3 states in the $Fe^{3+}(^6A_1)$–$Fe^{3+}(^6A_1)$ ground state manifold. The relative energies of the double-exciton states, relative to those of the ground and single-ion-excited-state manifolds, are shown in Figure 2.

Ligand to metal charge-transfer transitions

At energies higher than most of the ligand field transitions are the ligand to metal charge-transfer (LMCT) transitions. These are most easily described in terms of molecular orbital theory. The molecular orbital diagram for a $(FeO_6)^{9-}$ coordination polyhedron (Sherman, 1985) is shown in Figure 3. The lowest energy LMCT transitions are from non-bonding molecular orbitals (labelled $1t_{2u}$, $6t_{1u}$, and $1t_{1g}$ in Fig. 3) localized on the oxygen atoms to the antibonding t_{2g} Fe($3d$) orbitals. The energies of the $6t_{1u} \rightarrow 2t_{2g}$ and $1t_{2u} \rightarrow 2t_{2g}$ transitions are calculated to be 38,100 cm^{-1} and 43,600 cm^{-1}, respectively, in a $(FeO_6)^{9-}$

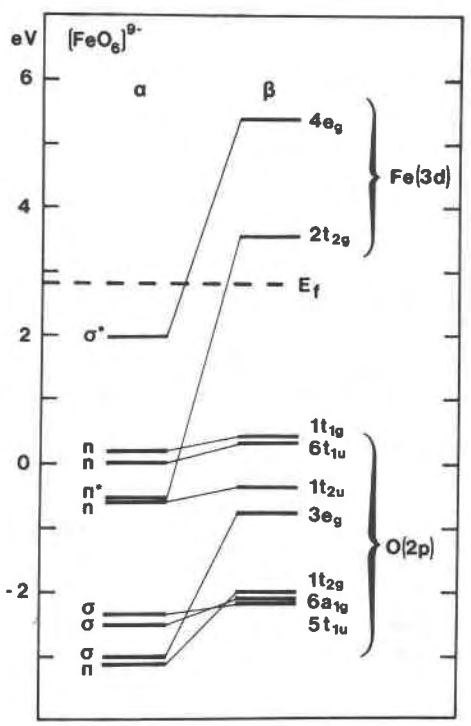

Fig. 3. Calculated molecular orbital diagram for an $(FeO_6)^{9-}$ cluster with an Fe–O bond length of 2.05Å (from Sherman, 1985). The α and β symbols refer to levels with spin-up (α-spin) or spin-down (β-spin). E_f is the Fermi energy, below which all orbitals are occupied in the ground state.

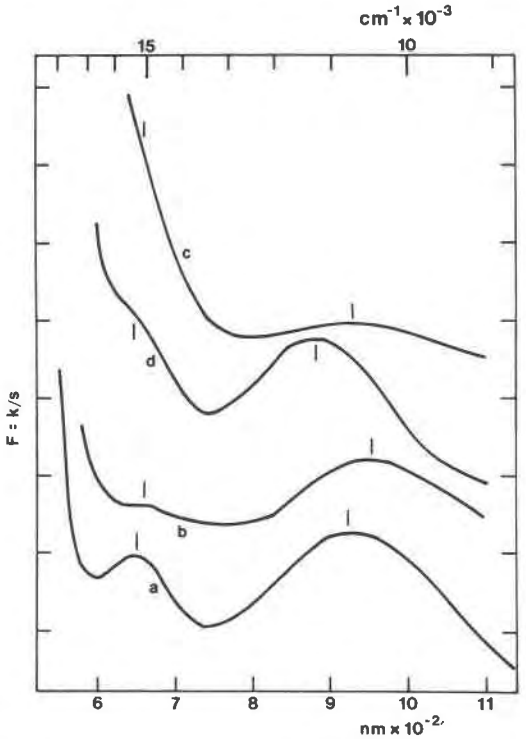

Fig. 4. Kebulka–Munk remission function (equation 1) of (a) goethite (b) lepidocrocite (c) maghemite (d) hematite in the visible and near-infrared regions as obtained from diffuse reflectance spectra. The vertical bars indicate band positions. The band near 900 nm corresponds to the $^6A_1 \rightarrow {}^4T_1(^4G)$ transition while the band near 640 nm corresponds to the $^6A_1 \rightarrow {}^4T_1(^4G)$ transition. The steep absorption edge in the visible region gives these minerals their yellow to red colors and results primarily from higher energy ligand field transitions which have been intensified by magnetic coupling of adjacent Fe^{3+} cations.

cluster with an Fe–O bond length of 2.05Å. Bands near these energies are observed in the spectra of several Fe^{3+} phyllosilicates (Chen et al., 1979; Karickhoff and Bailey, 1973), Fe^{3+}-oxo complexes (Lehman, 1970) and Fe^{3+} in Al_2O_3 (Tippins, 1970) and were also assigned to LMCT transitions. In the iron oxides, therefore, LMCT bands should be present near these energies.

Experimental

Except for hematite, all of the Fe_2O_3 and FeOOH samples were synthesized. The identity and purity of each sample was confirmed using powder X-ray diffraction and Mössbauer spectroscopy.

Lepidocrocite samples were prepared by aerial oxidation of a 0.01 M Fe(II) solution which was buffered to pH 6.5–7.5. The maghemite sample was synthesized by thermal dehydration of lepidocrocite. The product is a dark-brown magnetic powder. The 298 K Mössbauer spectrum of the sample used in this investigation showed a six-line hyperfine spectrum collapsing to a quadrupole doublet. This indicates that the mean particle size in this sample is sufficiently small to cause superparamagnetism. Small particle sizes are also indicated by the X-ray diffraction pattern where only the seven most intense lines for γ-Fe_2O_3 were observed and these were fairly broad and diffuse. Visible and near-ultraviolet absorption spectra were obtained using a Beckman model 25 spectrophotometer. Samples were dispersed in distilled water (pH = 4) using a sonifier and diluted to give a colloidal suspension of about 10 μM FeOOH or 5 μM Fe_2O_3. The spectra were obtained using a 5 cm length cell. Diffuse reflectance spectra in the visible and near-infrared were obtained using a Cary 17 spectrophotometer with an integrating sphere diffuse reflectance accessory. The integrating sphere was coated with MgO and the spectra were referenced against MgO. For easier comparison with the visible and near-ultraviolet absorption spectra, the reflectance spectra were converted to the Kebulka–Munk remission function defined by

$$F(R) = (1 - R)^2/2R = k/s \quad (3)$$

where R is the reflectance, k is the absorption coefficient and s is the scattering coefficient. Assuming that the scattering coefficient has only a small variation with wavelength over the range of

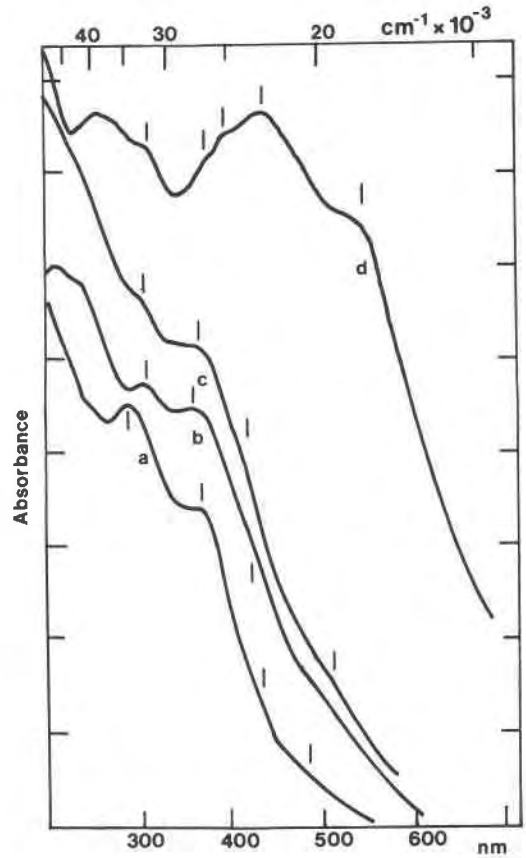

Fig. 5. Visible and near-ultraviolet absorption spectra of (a) goethite (b) lepidocrocite (c) maghemite and (d) hematite. Absorption bands near 430, 360–380, and 290–310 nm correspond to the $^6A_1 \rightarrow {}^4E$, $^4A_1(^4G)$, $^6A_1 \rightarrow {}^4E(^4D)$, and $^6A_1 \rightarrow {}^4T_1(^4P)$ ligand field transitions of Fe^{3+}. A feature near 485–550 nm is assigned to the $^6A_1 + {}^6A_1 \rightarrow {}^4T_1(^4G) + {}^4T_1(^4G)$ excitation of an Fe–Fe pair. Higher energy features, at wavelengths below 270 nm, are assigned to ligand-to-metal charge-transfer transitions.

interest, the shapes of the remission function and the actual absorption spectrum over that wavelength range should be identical.

Results and discussion

Figure 4 shows the visible and near-infrared diffuse reflectance spectra of the different iron oxides and oxide hydroxides. Near-UV and visible region absorption spectra of these minerals are shown in Figure 5. The visible and near ultraviolet spectra of goethite, lepidocrocite, and maghemite are all quite similar and, except for small differences in band energies qualitatively resemble the spectrum of the Fe^{3+} phyllosilicate nontronite investigated by Karickhoff and Bailey (1973). The shape of the hematite spectrum is quite different from those of the other iron oxides; the band energies in the hematite spectrum, however, are essentially the same. The primary difference between the hematite spectrum and the others is that a band at 430 nm in the hematite spectrum is quite intense while the analogous band in the spectra of maghemite and the FeOOH phases occurs only as an inflection. The reason for this will be discussed below. Note that the hematite spectrum obtained here is quite similar to the polarized absorption spectrum of a hematite thin film obtained by Marusek et al. (1980). The band energies in the two spectra, however, are somewhat different. This may be due to particle scattering in our spectrum or simply a dependence of the observed hematite band energies on the polarization direction in the single-crystal absorption spectrum.

In the near infrared and visible regions, all of the spectra are characterized by the presence of two prominent absorption bands near 640 nm (15,000 cm^{-1}) and 900 nm (11,000 cm^{-1}). These features can readily be assigned to the $^6A_1(^6S) \rightarrow {}^4T_2(^4G)$ and $^6A_1(^6S) \rightarrow {}^4T_1(^4G)$ ligand field transitions of Fe^{3+}, respectively. Analogous features were observed in the polarized absorption spectra of goethite and lepidocrocite single crystals obtained by Mao and Bell (1974). In the latter spectra, the splitting of the $^4T_2(^4G)$ band by the dynamic Jahn–Teller effect is quite evident; here, however, this phenomenon is unresolved. In principle, maghemite should contain some tetrahedrally coordinated Fe^{3+}; in the sample investigated here, however, the absorption bands can be accounted for by considering only transitions of octahedrally coordinated Fe^{3+}. Sherman (1985) argued that the $^6A_1 \rightarrow {}^4T_1(^4G)$ and $^6A_1 \rightarrow {}^4T_2(^4G)$ transitions of tetrahedrally coordinated Fe^{3+} should occur near 15,000 cm^{-1} and 19,500 cm^{-1}. Interference from such bands may explain why the $^6A_1 \rightarrow {}^4T_2(^4G)$ transition of octahedrally-coordinated Fe^{3+} (near 15,000 cm^{-1}) is so poorly resolved in the spectrum of γ-Fe_2O_3.

Additional spectral bands at wavelengths shorter than 600 nm are present in the diffuse reflectance spectra of all of the iron oxides and oxide hydroxides yet, because these transitions are so much more intense than the 640 and 900 nm bands, they give only a steep absorption edge. The visible region absorption spectra show two bands near 480–550 nm (20,800–18,180 cm^{-1}) and 430 nm (23,250 cm^{-1}). The former appears at 550 nm (18,180 cm^{-1}) and is a strong, reasonably well-defined feature in the spectrum of hematite. In the spectra of the other phases, however, the same band is at shorter wavelengths (480–500 nm) and is much weaker and gives only a slope change or small poorly-resolved peak. The 430 nm band is very strong and well-defined in hematite but gives only a perceptible shoulder in the spectra of the other minerals. The energy of the 430 nm feature (23,250 cm^{-1}) corresponds to that of the $^6A_1 \rightarrow {}^4E, {}^4A_1$ ligand field transition; the latter is about 22,000–23,000 cm^{-1} in the spectra of a wide variety of Fe^{3+} oxides, silicates, sulphates and phosphates (e.g., Lehmann, 1970; Manning, 1967; Manning, 1970). Given this assignment, the 480–550 nm band remains unaccounted for. This feature is absent in the spectra of minerals in which Fe^{3+} cations are not magnetically coupled to other Fe^{3+} ions. The lowest energy "double exciton" or pair excitation should occur near 440–480 nm and is the $^6A_1 + {}^6A_1 \rightarrow {}^4T_1(^4G) + {}^4T_1(^4G)$ transition. An analogous spectral band is found in Fe^{3+} doped Al_2O_3 (Ferguson and Fielding, 1972) and was also assigned to the pair excitation process. A second possible assignment for this band is that it is a split component (via the dynamic Jahn–Teller effect) of the $^4T_2(^4G)$ band. Such an assignment would imply a splitting of $\sim$5000 cm^{-1}, however, which seems unlikely. In hematite, goethite, and maghemite, the 480–550 nm (20,800–18,180 cm^{-1}) absorption bands that are assigned to the $^6A_1 + {}^6A_1 \rightarrow {}^4T_1(^4G) + {}^4T_1(^4G)$ double excition process are at energies somewhat less than twice that of the single ion $^6A_1 \rightarrow {}^4T_1(^4G)$ transition (22,600–20,800 cm^{-1}). (Note that the latter is more correctly designated as the $^6A_1 + {}^6A_1 \rightarrow {}^4T_1(^4G) + {}^6A_1$ "exciton + magnon" transition.) One might expect that the energy of a double exciton process would be given exactly by the sum of the energies of the component single ion transitions. The discrepancy can be explained with reference to the energy level diagram of Figure 2. For example, the energy required for the transition between the ground and excited pair states with $S = 2$ in the $^6A_1 + {}^6A_1 + {}^4T_1(^4G) + {}^6A_1$ exciton + magnon process, is found, using Equation 2, to be

$$E_1 = E_0 + (23/4)J_1 - (13/4)J_2 \quad (4)$$

Here, E_0 is the true energy of the $^6A_1 \rightarrow {}^4T_1(^4G)$ transition of a single, uncoupled, Fe^{3+} cation; J_1 is the exchange integral between two Fe^{3+} cations that are in the $^6A_1$ state; and J_2 is the exchange integral between an Fe^{3+} cation in the $^6A_1$ state and an Fe^{3+} cation in the $^4T_1(^4G)$ state. On the other hand, the energy required for the $^6A_1 + {}^6A_1 \rightarrow {}^4T_1(^4G) + {}^4T_1(^4G)$ double exciton transition ($S = 2$ states only) is

$$E_2 = 2E_0 + (23/4)J_1 - (3/4)J_3 \quad (5)$$

where J_3 is the exchange integral between two Fe^{3+} cations that are in the $^4T_1$ state. The difference between $2E_1$ and E_2 is then

$$\Delta E = (23/4)J_1 - (26/4)J_2 + (3/4)J_3 \quad (6)$$

If J_1, J_2 and J_3 are either very small or nearly equal, then

Table 2. Energies and assignments of bands observed in the Fe_2O_3 and FeOOH Spectra. Also given are the estimates for the ligand field theory parameters $10Dq$, B and C. The values in parentheses are the predicted transition energies based on the expressions given in Table 1.

	Observed (and calculated) electronic transition energies (1000/cm)			
Transition	Hematite	Goethite	Maghemite	Lepidocrocite
$^6A_1 \rightarrow {}^4T_1(^4G)$	11.3 (11.3)	10.9 (10.9)	10.7 (10.7)	10.4 (10.4)
$^6A_1 \rightarrow {}^4T_2(^4G)$	15.4 (15.4)	15.4 (15.3)	~15 (14.9)	15.4 (15.2)
$2(^6A_1) \rightarrow 2({}^4T_1(^4G))$	18.9	20.8	19.6	20.6
$^6A_1 \rightarrow {}^4E, {}^4A_1(^4G)$	22.5 (22.5)	~23 (23.3)	~23 (23.1)	~23 (23.5)
$\rightarrow {}^4T_2(^4D)$	24.7 (24.1)	-- (25.1)	-- (24.8)	-- (25.3)
$\rightarrow {}^4E(^4D)$	26.3 (26.3)	27.4 (27.4)	27.0 (27.0)	27.8 (27.8)
$\rightarrow {}^4T_1(^4P)$	31.3 (34.1)	35.0 (35.6)	31.7 (35.2)	32.8 (36.0)
$6t_{1u} \rightarrow 2t_{2g}$ (LMCT)	37.0	40.0	40.0	41.7
$1t_{2u} \rightarrow 2t_{2g}$ (LMCT)	--	44.4	--	47.6
	Estimated ligand field theory parameters (in cm^{-1})			
10Dq	14,000	15,320	15,410	15,950
B	540	590	560	610
C	3,410	3,490	3,510	3,470

ΔE would be close to zero. This may be the case in the binuclear Fe-EDTA complex investigated by Schugar et al. (1970) where the double exciton band energies are almost exactly equal to the sum of the component single ion transition energies. In general, however, the pair excitation bands will occur at energies only approximately equal to the sum of the component single ion transition energies. Depending on the values of J_1, J_2, and J_3, the difference between the pair excitation band energy and the sum of the single ion transition energies can be considerable. In binuclear oxo-bridged Fe^{3+} complexes, the magnitude of J_1 is on the order of 75–150 cm^{-1} (Murray, 1974). As such, values of ΔE on the order of 1,000–2,000 cm^{-1} are quite plausible.

The strong, well-defined band at 360–380 nm (27,780–26,300 cm^{-1}) is at an energy characteristic of the $^6A_1 \rightarrow {}^4E(^4D)$ transition. The $^6A_1 \rightarrow {}^4T_2(^4D)$ transition is of similar energy and it appears that in these spectra the two transitions are unresolved. The characteristic energies of the $^4E(^4D)$ and $^4T_2(^4D)$ states imply that, in the absorption spectra, they would only be separated by about 20 nm. In the spectrum of hematite, however, the two transitions appear to be resolved with the $^4E(^4D)$ state at 380 nm (26,300 cm^{-1}) and the $^4T_2(^4D)$ state at 405 nm (24,700 cm^{-1}). A very strong band near 290–310 nm (34,480–32,260 cm^{-1}) is tentatively assigned to the $^6A_1 \rightarrow {}^4T_1(^4P)$ ligand field transition. There are several alternative assignments for this band, however. The first is to the pair excitation $^6A_1 + {}^6A_1 \rightarrow {}^4T_1(^4G) + {}^4E, {}^4A_1(^4G)$; from the single ion transition energies, this is predicted to have an energy of 33,800–34,200 cm^{-1}. A second alternative assignment is the pair excitation $^6A_1 + {}^6A_1 \rightarrow {}^4T_2(^4G) + {}^4T_2(^4G)$ which should have an energy near 30,800 cm^{-1}. The observed peak may, in fact, be a composite of these three transitions. Note that the visible to near-ultraviolet spectrum of maghemite is quite similar to that of the FeOOH phases even though the former should contain some tetrahedrally-coordinated Fe^{3+}. The higher energy, and nominally field independent, ligand field states of tetrahedrally coordinated Fe^{3+} have energies which are similar to the analogous states of octahedrally coordinated Fe^{3+}. As such, bands attributable to Fe^{3+} in octahedral and tetrahedral coordination may not be resolved in Figure 5.

At wavelengths shorter than about 270 nm, there are several broad bands which can readily be assigned to LMCT transitions. The energies of these absorption bands are similar to those of analogous bands in other Fe^{3+} oxides, silicates and inorganic complexes involving Fe–O bonds (e.g., Karickhoff and Bailey, 1973; Tippins, 1970; Lehman, 1970). In most of the spectra reported here, the LMCT bands are rather ill-defined. This may be due to increased light scattering at shorter wavelengths.

The observed band energies and their assignments are summarized in Table 2. From the $^6A_1 \rightarrow {}^4T_1(^4G)$, $^6A_1 \rightarrow {}^4E$,

$^4A_1(^4G)$, and $^6A_1 \rightarrow {}^4E(^4D)$ transition energies and the Tanabe–Sugano equations (Table 1), we can calculate values for the ligand field theory parameters $10Dq$, B and C and use these to predict the energies of the remaining transitions. The values for $10Dq$, B, and C, together with the predicted band energies, are summarized in Table 2. The predicted energies of the pair excitation bands are obtained assuming that they are equal to the sum of the two ligand field transition energies. As discussed previously, this may sometimes be only a rough approximation.

The values for $10Dq$, B, and C are physically quite reasonable and are similar to those obtained in other Fe^{3+} oxygen systems. The values for $10Dq$ agree with that obtained (15,800 cm^{-1}) from the SCF-Xα-SW calculation on an $(FeO_6)^{9-}$ cluster (Sherman, 1985). The energy of the $^6A_1 \rightarrow {}^4T_2(^4G)$ band is predicted quite accurately. Finally, the energies of the LMCT transitions are in good agreement with the energies obtained from the $(FeO_6)^{9-}$ molecular orbital calculations. These considerations support the overall band assignments given in Table 2. Note, however, that the predicted energy of the $^4T_1(^4P)$ band is in rather poor agreement with that observed. This is to be expected. First, the energy of this excited state is most likely depressed by configurational interaction with the LMCT excited states with T_1 symmetry. Second, the Tanabe–Sugano expression used to calculate this state energy is only approximate. Third, as mentioned above, the observed band may instead be due to the $^6A_1 + {}^6A_1 \rightarrow {}^4T_1(^4G) + {}^4E$, $^4A_1(^4G)$ and $^6A_1 + {}^6A_1 \rightarrow {}^4T_2(^4G) + {}^4T_2(^4G)$ double exciton processes.

The $(FeO_6)^{9-}$ molecular orbital calculations cannot predict the energies of the individual ligand field transitions. Such calculations can, however, estimate the average energy of the ligand field states that arise from a given electronic configuration. The calculation on the $(FeO_6)^{9-}$ cluster (Sherman, 1984) estimates that the average energy of the quartet states arising from the $(t_{2g})^3(e_g)^2$ configuration is 30,500 cm^{-1}. We cannot directly estimate the average energy of these states from the spectra because the energy of the $^4A_2(^4F)$ state is unknown. Using the values for B and C, however, we can estimate the average energy of these states using the Tanabe–Sugano expressions for the state energies (Table 1). This gives 27500, 28300, 28400 and 28900 cm^{-1} for hematite, goethite, maghemite, and leipidocrocite, respectively. These are in good agreement with the theoretical result and add further support both to the band assignment scheme and to the reliability of the molecular orbital calculations.

A rather different, but at first glance reasonable, band assignment scheme would be to assign the 480–550, 430, and 360–380 nm bands to the $^6A_1 \rightarrow {}^4E$, $^4A_1(^4G)$, $^6A_1 \rightarrow {}^4T_2(^4D)$, and $^6A_1 \rightarrow {}^4E(^4D)$ transitions, respectively. This scheme, however, gives an unrealistically small value for $10Dq$ ($\sim$9000 cm^{-1}) and B values which are greater than the Fe^{3+} free ion value. Also, the resulting $10Dq$, B and C values give a poor prediction of the $^6A_1 \rightarrow {}^4T_2(^4G)$ transition energy.

Given the assignments of the bands at wavelengths greater than 270 nm to Fe^{3+} ligand field and pair excitation processes, it is significant that their intensities are comparable to those of the LMCT bands. In the iron oxides and oxide hydroxides, the spin and Laporte selection rules for the Fe^{3+} ligand field transitions are relaxed by the magnetic coupling of adjacent Fe^{3+} cations. This magnetic coupling occurs via the superexchange interaction which, in turn, results from the spin polarization of the Fe–O chemical bond. All of these minerals have FeO_6 coordination polyhedra in edge- and corner-sharing arrangements which allow relatively strong magnetic coupling via superexchange interactions. In hematite, however, FeO_6 polyhedra are also in face-sharing arrangements. The face-sharing arrangement results in a trigonal distortion of the FeO_6 coordination polyhedra. Molecular orbital calculations on octahedral and trigonally-distorted FeO_6 coordination polyhedra (Sherman, 1985) show that the trigonal distortion increases the spin-polarization of the oxygens bridging face-sharing FeO_6 polyhedra. This, in turn, implies that the superexchange interaction and, hence, the strength of the magnetic coupling, between face-sharing FeO_6 polyhedra in hematite will be greater than that between the edge-sharing FeO_6 polyhedra in the other oxides and oxide hydroxides. Accordingly, we expect the Fe^{3+} ligand field transitions in hematite to be more intense than those in the other iron oxides. On the other hand, the strength of the coupling between two Fe^{3+} cations will vary depending on the electronic states of the Fe^{3+} cations; that is, some Fe^{3+} ligand field transitions will be intensified much more so than others. This is why the shape of the hematite spectrum is so different from that of the other iron oxides: the $^6A_1 \rightarrow {}^4E$, $^4A_1(^4G)$ transition in hematite is strongly intensified by the greater degree of Fe^{3+}–Fe^{3+} coupling. The $^6A_1 + {}^6A_1 \rightarrow {}^4T_1 + {}^4T_1$ pair excitation feature near 550 nm is also much stronger. The most noticeable effect of the stronger Fe^{3+}–Fe^{3+} coupling in hematite, relative to the other iron oxides, is that the former is deep red while the latter are pale yellow to brown. Rossman (1975; 1976) has shown how the colors of Fe^{3+} sulphate and phosphate minerals can be directly related to their magnetic structures.

Summary and conclusions

Near-infrared to near-ultraviolet spectra of Fe(III) oxides and oxide hydroxides show bands due to ligand field and ligand-to-metal charge-transfer transitions whose energies are similar to those found in other Fe(III) oxygen systems. The Fe^{3+} ligand field transitions are strongly intensified by magnetic coupling of adjacent Fe^{3+} cations in the crystal structures of these minerals. Additional spectral features are attributed to the simultaneous excitation of two Fe^{3+} cations which are magnetically coupled. From the spectra and the band assignment scheme, values for the ligand field theory parameters $10Dq$, B and C were calculated. The parameters are physically reasonable and are able to accurately predict the energies of the Fe^{3+} ligand field transitions. A comparison with the spectral band energies and the results of spin-polarized SCF-Xα-SW molecular orbital

calculations on Fe^{3+} coordination sites in oxides show very good agreement. The theoretical value for $10Dq$ was calculated to be 15,800 cm^{-1}; this compares well with the experimental values which range from 14,000 to 15,950 cm^{-1}. The one-electron molecular orbital calculations estimate that average energy of the quartet ligand field states arising from the $(t_{2g})^3(e_g)^2$ configuration to be 30,500 cm^{-1}. From the experimental values for B and C, the average energies of these states is estimated to be 27,500 to 29,000 cm^{-1}, in good agreement with the MO calculations. The SCF-Xα-SW calculations give the energies of the first few ligand to metal charge-transfer transitions to be 38,100 and 43,600 cm^{-1}. In the iron oxide and oxide hydroxide spectra, these transitions are found at 37,000–41,700 cm^{-1} and 44,400–47,600 cm^{-1}.

Taken together, these results show that the ligand-to-metal charge transfer transitions in Fe^{3+} oxides and silicates occur at energies much higher than those suggested by some previous investigators. The visible region absorption edge, which gives the iron oxides their red to yellow colors, does not result from ligand-to-metal charge-transfer transitions but is a consequence of very intense Fe^{3+} ligand field and Fe^{3+}–Fe^{3+} pair transitions. Both types of transitions are Laporte and spin-allowed via the magnetic coupling of adjacent Fe^{3+} cations.

Acknowledgments

We would like to thank R. G. Burns for helpful comments and suggestions regarding the manuscript. This work was supported by NASA Grant no. NSG-7604 and NSF Grant no. EAR-8313585 awarded to R. G. Burns.

References

Chen, Y., Shaked, D., and Banin, A. (1979) The role of structural iron in the UV absorption by smecites. Clay Minerals, 14, 93–102.

Ferguson, J., Guggenheim, H. J., and Tanabe, Y. (1966) The effects of exchange interactions in the spectra of octahedral manganese II compounds. Journal of the Physical Society of Japan, 21, 347–354.

Ferguson, J. and Fielding, P. E. (1972) The origins of the colours of natural yellow, blue, and green sapphires. Australian Journal of Chemistry, 25, 1371–1385.

Karickhoff, S. W., and Bailey, G. W. (1973) Optical absorption spectra of clay minerals. Clays and Clay Minerals, 21, 59–70.

Krebs, J. J. and Maisch, W. G. (1971) Exchange effects in the optical absorption spectra of Fe^{3+} in Al_2O_3. Physical Review B, 4, 757–769.

Lehmann, G. (1970) Ligand field and charge transfer spectra in Fe(III)–O complexes. Zeitschrift für Physikalische Chemie Neue Folge, 72, 279–297.

Lehmann, G., and Harder, H. (1970) Optical spectra of di- and trivalent iron in corundum. American Mineralogist, 55, 98–105.

Lever, A. B. P. (1968) Inorganic Electronic Spectroscopy. Elsevier, Amsterdam.

Lohr, L. L. (1972) Spin-forbidden electronic excitations in transition metal complexes. Coordination Chemistry Reviews, 8, 241–259.

Manning, P. G. (1967) The optical absorption spectra of some andradites and the identification of the $^6A_1 + {}^4A_1$, ^4E transition in octahedrally bonded Fe^{3+}. Canadian Journal of Earth Sciences, 4, 1039–1047.

Manning, P. G. (1970) Racah parameters and their relationship to lengths and covalencies of Mn^{2+} and Fe^{3+} oxygen bonds in silicates. Canadian Mineralogist, 10, 677–687.

Mao, H. K. and Bell, P. M. (1974) Crystal-field effects of ferric iron in goethite and lepidocrocite: band assignments and geochemical application at high pressure. Carnegie Institute of Washington Yearbook, 1973, 502–507.

Marusak, L. A., Messier, R. and White, W. B. (1980) Optical absorption spectrum of hematite, α-Fe203, near IR to UV. Journal of Physics and Chemistry of Solids, 41, 981–984.

Murray, K. S. (1974) Binuclear oxo-bridged iron(III) complexes. Coordination Chemistry Reviews, 12, 1–35.

Rossman, G. R. (1975) Spectroscopic and magnetic studies of ferric iron hydroxy sulphates: intensification of color in ferric iron clusters bridged by a single hydroxide ion. American Mineralogist, 60, 698–704.

Rossman, G. R. (1976) Spectroscopic characteristics and magnetic studies of ferric iron hydroxyl sulphates—the series $Fe(OH)SO_4 \cdot nH_2O$ and the jarosites. American Mineralogist, 61, 398–404.

Schugar, H. J., Rossman, G. R., Thibeault, J. and Gray, H. B. (1970) Simultaneous pair electronic excitations in a binuclear iron(III) complex. Chemical Physics Letters, 6, 26–28.

Sherman, D. M. (1985) Electronic structures of Fe^{3+} coordination sites in iron oxides: applications to spectra, bonding, and Magnetism. Physics and Chemistry of Minerals, 12, 161–175.

Sherman, D. M., Burns, R. G. and Burns, V. M. (1982) Spectral characteristics of the iron oxides with application to the Martian bright region mineralogy. Journal of Geophysical Research, 87, 10169–10180.

Singer, R. B. (1982) Spectral evidence for the mineralogy of high albedo soils and dusts on Mars. Journal of Geophysical Research, 87, 10159–10168.

Singer, R. B., McCord, T. B., Clark, R. N., Adams, J. B. and Huguenin, R. L. (1979) Mars surface composition from reflectance spectroscopy: a summary. Journal of Geophysical Research, 84, 8415–8426.

Strens, R. G. J. and Wood, B. J. (1979) Diffuse reflectance spectra and optical properties of some iron and titanium oxides and oxyhydroxides. Mineralogical Magazine, 43, 347–354.

Tippins, H. H. (1970) Charge-transfer spectra of transition metal ions in cordundum. Physical Review B, 1, 126–135.

Waite, T. D. (1983) Photoredox Properties of Iron in Natural Waters. Ph.D. dissertation, Massachusetts Institute of Technology.

Manuscript received, October 23, 1984; accepted for publication, July 29, 1985.